Phosphorylation of Nucleoside Diphosphate Kinase at the Active Site Studied by Steady-State and Time-Resolved Fluorescence†

Dominique Deville-Bonne,*,‡ Olivier Sellam,§ Fabienne Merola,|| Ioan Lascu,§,⊥ Michel Desmadril,‡ and Michel Véron§

Laboratoire de Modélisation et d'Ingéniérie des Protéines, Université Paris-Sud Orsay, bat 430, 91405 Orsay Cedex, France, Unité de Régulation Enzymatique des Activités Cellulaires, CNRS URA 1149, Institut Pasteur, 25 rue du Dr Roux, 75724 Paris Cedex 15, France, and Laboratoire pour l'Utilisation du Rayonnement Electromagnétique, CNRS-MEN-CEA, Université Paris-Sud, 91405 Orsay Cedex, France

Received April 18, 1996; Revised Manuscript Received July 8, 1996⊗

ABSTRACT: Nucleoside diphosphate (NDP) kinase is the enzyme responsible in the cell for the phosphorylation of nucleoside or deoxynucleoside diphosphates into the corresponding triphosphates at the expense of ATP. Transfer of the γ-phosphate is very fast (turnover number above 1000 s^{-1}) and involves the phosphorylation of a histidine residue at the active site of the enzyme. We have used intrinsic protein fluorescence of the single tryptophan of *Dictyostelium discoideum* NDP kinase as a sensitive probe for monitoring the interaction of the enzyme with its substrates. We demonstrate that the 20% quenching of steady-state fluorescence observed upon addition of ATP is due to formation of the phosphorylated intermediate. Time-resolved fluorescence indicates that the Trp-137 side chain is rigidly bound to the protein core with a unique lifetime of 4.5 ns for the free enzyme at 20 °C and that it remains tightly immobilized during the time course of the reaction. Phosphorylation of this catalytic residue (His-122) in the presence of ATP induces a similar decrease in mean lifetime, due to the splitting of the signal and the appearance of a shorter decay. This splitting is discussed in terms of a slow conformational equilibrium. We demonstrate that, in the wild-type enzyme, the conserved His-55 quenches the fluorescence of Trp-137 as the H55A mutant protein fluorescence displays an increase in quantum yield. Even though H55A mutant enzyme is active, the absence of the imidazole ring prevents the detection of the phosphorylated state of His-122 by Trp-137. We conclude that His-55 serves as a relay between His-122 and Trp-137.

Nucleoside diphosphate (NDP)[1] kinase (EC 2.7.4.6) catalyzes the exchange of phosphate between a nucleotide triphosphate (especially ATP) and a nucleoside diphosphate according to a mechanism which involves a phosphorylated histidine intermediate (Parks & Agarwal, 1973). The enzyme is able to phosphorylate both ribo- and deoxyribonucleotides and shows no specificity towards the base. NDP kinase follows a ping-pong bi-bi mechanism (Garces & Cleland, 1969): the overall reaction is the sum of donor and acceptor half-reactions, according to the following scheme:

$$\text{ATP} + \text{E} \Leftrightarrow \text{E-P} + \text{ADP} \quad (1A)$$

$$\text{NDP} + \text{E-P} \Leftrightarrow \text{NTP} + \text{E} \quad (1B)$$

Although NDP kinase was purified almost 30 years ago, the cloning of its gene is relatively recent (Lacombe *et al.*, 1990; Munoz-Dorado *et al.*, 1990). NDP kinase was also identified as the product of the genes *awd* from *Drosophila* (Dearolf *et al.*, 1988) and *nm23* from human (Rosengard *et al.*, 1989; Steeg *et al.*, 1988) involved in larval development and metastasis, respectively, suggesting that NDP kinase may not be considered only as a "housekeeping" enzyme. NDP kinases are conserved throughout evolution, with 40% and 62% sequence identity, respectively, for the enzymes of *Escherichia coli* and of *Dictyostelium* as compared to that from human (Gilles *et al.*, 1991, Wallet *et al.*, 1990).

The three dimensional structure of the NDP kinase from *Dictyostelium* (Dumas *et al.*, 1992), from *Myxococcus* (Williams *et al.*, 1993), from *Drosophila* (Chiadmi *et al.*, 1993), and from human (Morera *et al.*, 1995b; Webb *et al.*, 1995) have been determined by X-ray crystallography. All eukaryotic NDP kinases are hexamers made of identical 17-kDa subunits. Their structure is highly similar, in particular around the active site. The structures of *Dictyostelium* NDP kinase complexed to a purine nucleotide (ADP) (Morera *et al.*, 1994b) and to a pyrimidine nucleotide (dTDP) (Cherfils *et al.*, 1994) are remarkably similar to that of the free enzyme. The mode of nucleotide diphosphate binding is original, as the base stacks on the aromatic ring of Phe-64 near the protein surface while the sugar and the phosphate chain are deeper inside the active site and interact with

† This work was supported by funds from Agence Nationale de la Recherche contre le SIDA (ANRS AC 14), from Association de la Recherche contre le Cancer (ARC 6438) and from the Ligue contre le Cancer (Comité de Paris) to M.V.

* Corresponding author. Present address: Unité de Régulation Enzymatique des Activités Cellulaires, CNRS URA 1149, Institut Pasteur, 25 rue du Dr. Roux, 75724 Paris Cedex 15, France.

‡ Laboratoire de Modélisation et d'Ingéniérie des Protéines, Université Paris-Sud Orsay.

§ Institut Pasteur.

|| Laboratoire pour l'Utilisation du Rayonnement Electromagnétique, Université Paris-Sud.

⊥ Present address: Université Bordeaux II, IBGC-CNRS, 1 rue Camille Saint-Saens, 33077 Bordeaux Cedex, France.

⊗ Abstract published in *Advance ACS Abstracts,* November 1, 1996.

[1] Abbreviations: NATrA, *N*-acetyltryptophanamide; BSA, bovine serum albumine; NDP, nucleoside diphosphate; NTP, nucleoside triphosphate.

S0006-2960(96)00945-2 CCC: $12.00

numerous side chains of the protein and a magnesium ion. A set of H-bonds is responsible for the particular conformation of the nucleotide: the 3′OH of the (deoxy)ribose participates to H-bonds with Lys-16 and Asp-119 as well as with an oxygen of the β-phosphate. The X-ray structure of the phosphorylated intermediate shows no major change relative to free proteins (Morera *et al.*, 1995a). A study of the active site by site-directed mutagenesis (Tepper *et al.*, 1994) supports the proposed model for phosphate transfer to the catalytic His-122 (Morera *et al.*, 1995a), suggesting that catalysis can proceed with little induced fit, which might be essential for an enzyme with a very high turnover number.

The fluorescence of the single tryptophan residue in the *Dictyostelium* enzyme, Trp-137, has been shown to decrease upon unfolding of the protein and was used to monitor equilibrium dissociation and unfolding transitions of NDP kinase in urea (Lascu *et al*., 1993, 1994). We show here that Trp-137 is also a suitable intrinsic probe near the catalytic core of *Dictyostelium* NDP kinase. We have measured the interactions of NDP kinase with nucleotides by steady-state intrinsic fluorescence spectroscopy and time-resolved fluorescence using synchrotron radiation. This latter approach provides information concerning Trp-137 side-chain dynamics. The structural basis of the effects of nucleotides on tryptophan fluorescence has also been investigated using the H55A mutant NDP kinase.

EXPERIMENTAL PROCEDURES

Materials. ATP, lactate dehydrogenase, and pyruvate kinase were from Boehringer Mannheim. dTDP and NATrA were from Sigma, and ultrapure urea was from ICN Biomedicals, Inc. [γ-^{32}P]ATP (4500 Ci/mmol) was from Amersham.

Site-Directed Mutagenesis. Mutant H55A and H122Q *Dictyostelium* NDP kinase were made by site directed mutagenesis according to Kunkel (1985), and the mutations were verified by standard DNA sequencing techniques. The oligonucleotides used for mutagenesis were 5′-AGCT-GAATCT**GC**CTATGCTGAA-3′ for H55A mutant and 5′-CATCATCCA**A**GGTTCTGATTC-3′ for H122Q mutant. Altered bases as compared to the wild-type sequence are underlined. Mutant H122C NDP kinase was described in Dumas *et al.* (1992).

Enzyme Purification and Activity Assays. Mutant and wild-type *Dictyostelium* NDP kinases were overexpressed in *E. coli* (XL1-Blue) using plasmid *pndk* as described (Lacombe *et al.*, 1990). The cell extract was loaded at pH 8.4 onto DEAE-Sephacel which retained only *E. coli* NDP kinase (Tepper *et al.*, 1994). The flowthrough was adsorbed on Blue-Sepharose (Pharmacia) at pH 7.5. After a wash with 0.3 M NaCl, the enzyme was eluted by 1.5 M NaCl in Tris-HCl buffer, pH 7.5. After dialysis, the protein was concentrated with an Amicon ultrafiltration cell and stored frozen at −20 °C. Protein concentration was determined in the spectrophotometer using an absorbance coefficient of $\Delta A_{280} = 0.55$ for a 1 mg/mL solution. Mutant proteins were purified according to the same procedure. The absorption coefficient of wild-type enzyme was also used for H122C, H122Q, and H55A mutant proteins.

The activity of NDP kinase was measured at 20 °C using a coupled assay as previously described (Lascu *et al.*, 1992). NDPK concentration is expressed as that of subunit concentration using $M_W = 17\,000$.

Phosphorylated Enzyme. The incorporation of radioactive phosphate from [γ-^{32}P]ATP into the protein was measured after a 5-min incubation of 15 μM enzyme with 90 μM [γ-^{32}P]ATP (0.5 Ci/mmol). The mixture was then gel-filtered on a 12-mL G25 Sephadex column equilibrated with buffer T (50 mM Tris-HCl buffer, pH 7.5, containing 5 mM $MgCl_2$ and 75 mM KCl). The enzyme was separated from nucleotides and free phosphate by elution with buffer T. The radioactivity and the protein concentration were then measured in each fraction and the stoichiometry of phosphate incorporation was calculated.

Stability Measurements. Thermal inactivation experiments were performed according to Lascu *et al.* (1992) on pure recombinant protein at the concentration of 5 μM in 50 mM Tris acetate buffer, pH 7.4, containing 1 mg/mL BSA. Samples were incubated at the appropriate temperature for 10 min and kept on ice for 30 min before measurement of the residual activity.

For inactivation by urea, pure recombinant protein (3 μM) was incubated at 25 °C for 24 h in 50 mM Tris acetate buffer, pH 7.4, containing various concentrations of urea. The amount of activity was measured by transferring the protein into the standard assay. We verified that the residual urea concentration (less than 80 mM) did not interfere with the activity assay. No significant reactivation occurred during the measurement.

Steady-State Fluorescence. All fluorescence measurements were performed at 20 °C in 50 mM Tris-HCl buffer, pH 7.5, containing 5 mM $MgCl_2$ and 75 mM KCl (buffer T) on a SLM 8000 spectrofluorometer. The excitation wavelength was 295 nm to minimize the contribution of tyrosyl residues to the total fluorescence as well as light absorption by ATP. The excitation and emission bandwidths were both set to 2 nm. Rhodamine was used to correct for fluctuations of the excitation light. The spectra were corrected by subtracting background intensities of a blank solution made of buffer solution with the added nucleotide.

Fluorescence quantum yields were determined according to the method of Parker and Rees (1960), using the equation

$$QY_{prot} = \frac{I_{prot} A_{NATrA}}{I_{NATrA} A_{prot}} QY_{NATrA} \qquad (2)$$

where I is the integrated intensity over the wavelength region 305−480 nm and A is the absorbance at 295 nm. The quantum yield of NATrA was shown to be identical to that of tryptophan at pH 7, 20 °C: $QY_{NATrA} = QY_{Trp} = 0.14$ (Werner & Foster, 1979; Szabo & Rayner, 1980).

Time-Resolved Fluorescence Measurements. The fluorescence decays were measured by the single photoelectron counting method, using the synchrotron radiation of SUPER-ACO at Laboratoire pour L'Utilisation du Rayonnement Electromagnetique (LURE, Orsay) as a pulsed excitation light. This storage ring provides a light pulse of approximatly 600 ps (full width at half-maximum) at a frequency of 8.3 MHz for a double-bunch mode. The optical and electronic parts of the instrumental setup were described elsewhere (Brochon *et al*., 1993). A Hamamatsu microchannel plate R1564U-06 was used as detector. Unless otherwise indicated, the excitation and emission wavelengths were respectively set at 300 and 340 nm with Jobin-Yvon

H25 monochromators with bandwidths of 4.5 and 9 nm, respectively. Time sampling was 25 ps/channel, and 2048 channels were used. The fluorescence of a 1-mL sample was measured in a 5 × 10 mm quartz cuvette. Data for the measured parallel $I_{vv}(t)$ and the perpendicular $I_{vh}(t)$ components of the fluorescence intensity, as well as the instrumental function $E_\lambda(t)$, were measured alternately and stored in separate memories of a plug-in multichannel analyzer card (Canberra). Routinely about $2-3 \times 10^7$ counts were stored for the total fluorescence $[I_{vv}(t) + 2\beta I_{vh}(t)]$ intensity decay. The response function of the instrument was determined by measuring the light scattered by a Ludox solution at the emission wavelength.

The correction factor β for the polarization bias was determined from the depolarized fluorescence of NATrA at 20 °C under identical optical conditions:

$$\beta(\lambda_{em}) \equiv \frac{\int_{t_0}^{\infty} I_{vv}(t)\, dt}{\int_{t_0}^{\infty} I_{vh}(t)\, dt} \tag{3}$$

t_0 being the time at which the fluorescence of NATrA is fully depolarized. The relative level of scattered light present in the fluorescence signal was found to be undetectable (i.e., less than 0.1%), as checked with a Ludox solution observed under the conditions normally used for fluorescence detection.

The total intensity decay was analyzed by the maximum entropy method (Livesey & Brochon, 1987) using the FAME program (MEDC Ltd., U.K.) after summing the parallel and the perpendicular component according to

$$T(t) = I_{vv}(t) + 2\beta I_{vh}(t) = E_\lambda(t) \int_0^{\infty} \alpha(\tau) e^{-t/\tau} \tag{4}$$

where $\alpha(\tau)$ is the fluorescence lifetime distribution. The quality of the fits was judged by the randomness of the weighed residuals and the low value of the reduced χ^2. All details of the analysis procedure are given in Blandin *et al.* (1994). A total number of 120 iterations was systematically performed.

The mean lifetime is the first-order average

$$\bar{\tau} = \sum_i \alpha_i \tau_i \tag{5}$$

computed from all elementary amplitudes and lifetimes of the distribution.

Polarized light excites preferentially the absorption dipoles that are oriented more nearly parallel to the direction of the exciting electric vector. The anisotropy $r(t)$ is most usefully defined by

$$r(t) \equiv \frac{I_{vv}(t) - \beta I_{vh}(t)}{I_{vv}(t) + 2\beta I_{vh}(t)} \tag{6}$$

where $I_{vv}(t)$ and $I_{vh}(t)$ are the intensities decay laws of the polarized emission light parallel and perpendicular, respectively, to an infinitely short pulse of vertically polarized excitation light.

The time dependency of the anisotropy that is related to the average orientation of the emission moment with respect to the excitation polarization is

$$r(t) = \sum_i A_i \epsilon^{(-\tau/\theta_i)} \tag{7}$$

where θ_i is the rotational correlation times and $\Sigma_i A_i = r_0$, the fluorescence anisotropy extrapolated at zero time, which, in the absence of fast depolarization processes, should approach the fundamental value of 0.300 expected for tryptophan excited at 300 nm (Valeur & Weber, 1977). For a rigid sphere in a homogeneous medium, the relaxation time can be equated to the rotational correlation time for the tumbling of the molecule and is described by the Stokes−Einstein relation:

$$\theta = \frac{\eta V}{kT} \tag{8}$$

η being the viscosity of the solvent, V the volume of the sphere, T the absolute temperature, and k the Boltzmann constant. The fluorescence anisotropy decays were analyzed in a one-dimensional way using the maximum entropy method as detailed previously (Blandin *et al.*, 1994).

RESULTS

Fluorescence Properties of NDP Kinase Trp-137. At an excitation wavelength of 295 nm, the steady-state intrinsic fluorescence of *Dictyostelium* NDP kinase at 20 °C, pH 7.5, is primarily due to its single tryptophan residue, Trp-137 (Figure 1, curve B). The quantum yield is 0.27 (Table 1), assuming a quantum yield of 0.14 for NATrA (Werner & Foster, 1979). The wavelength of maximum emission of NDP kinase is shifted to the blue as compared to NATrA (Figure 1, curve D), and the full width at half-maximum of the spectrum is lower than that of NATrA (49 vs 61 nm).

The time-resolved fluorescence spectroscopy of NDP kinase provides information about the dynamics and the possible conformational changes of the protein. At 20 °C, the fluorescence lifetime distribution obtained with the wild-type NDP kinase displayed a major component (90%) centered at 4.6 ns and two minor components (around 5% each) at 3.4 and 0.3 ns, resulting in a mean lifetime of 4.36 ns with a quasi-homogeneity in fluorescence intensity (Figure 2a, Table 1). In all measurements, a short lifetime (0.3−0.4 ns) is found in a constant low amount (6−7% of the distribution).

The fluorescence anisotropy decays of NDP kinase at 20 °C were measured under the same conditions. They are satisfactorily described by single-exponential functions with similar relaxation times (65 ± 20 ns) consistent with a stable, nearly spherical hexamer (Table 2). A significant difference was found for the P105G mutant NDP kinase, which dissociates easily into folded monomers in the presence of low urea concentrations (Lascu *et al.*, 1993, 1994). According to the Stokes−Einstein relationship (eq 8), the theoretical values for rotational diffusion coefficient are 9, 18, and 55 ns for globular proteins of M_w = 17 000, 2 × 17 000 and 6 × 17 000, respectively, assuming an additional hydration volume of 75%, which gives good agreement with many experimental observations on small globular proteins (Wahl, 1980; Kouyama *et al*., 1989; Blandin *et al*., 1994). Indeed, in the case of the P105G mutant, 4% of a 7 ns ± 1 ns correlation time species is found, which can be attributed to the NDP kinase monomer.

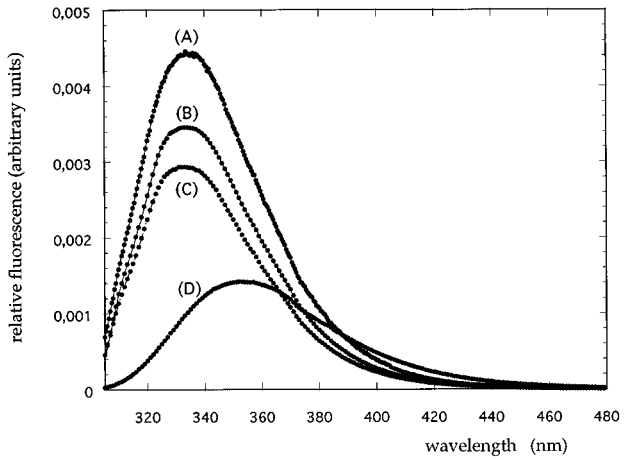

FIGURE 1: Fluorescence emission spectra of NDP kinase. The emission spectra of wild-type and H55A mutant protein in buffer T are compared to that of NATrA (λ_{exc} = 295 nm). Spectra were corrected by the SLM procedure. Proteins and NATrA concentrations were adjusted in order that A_{295} = 0.1. (A) H55A mutant NDP kinase, (B) wild-type NDP kinase, (C) phosphorylated NDP kinase, and (D) NATrA.

In all cases, the anisotropy decays were devoid of any constant term r_∞, showing the absence of higher molecular weight components or aggregates in the samples (Merola *et al.*, 1995). Another informative parameter is the initial anisotropy obtained by extrapolation at zero time (r_0). In our samples, r_0 is close to 0.3, as expected for an immobilized tryptophan (Valeur & Weber, 1977).

Substrate Effects on NDP Kinase Fluorescence. Although Trp 137 is not located in the active site, its fluorescence is affected by addition of ATP. The addition of saturating amounts of ATP results in a strong decrease of fluorescence (22%) without noticeable modification of the maximum emission wavelength (Figure 3). This quenching could be due either to the binding of nucleotide or to phosphorylation of His-122 (eq 1A). As shown in Figure 3, the nonhydrolyzable ATP analogs AMP-PNP and AMP-PCP have no effect, while ADP produces less than 5% attenuation of the signal, indicating that the fluorescence quenching is due to phosphorylation of the enzyme rather than nucleotide binding *per se*. This is further demonstrated by the fact that the fluorescence of the inactive enzymes H122C and H122Q, mutated on the catalytic histidine, is not affected by nucleotides (data not shown).

Studies using the phosphorylated enzyme indicate also that the quenching of fluorescence is due to phosphorylation.The phosphorylated intermediate was prepared by incubation of wild-type NDP kinase with an excess of ATP as described under Experimental Procedures. Using [γ-^{32}P]ATP under the same conditions, we verified that one phosphate was incorporated per active site (data not shown). The half-life of the phosphoenzyme (about 2 h under the conditions used; Bominaar *et al.*, 1994; Lecroisey *et al.*, 1995) allows us to study its fluorescence. The fluorescence intensity decreased relative to that of free enzyme by about 20% (Figure 1 and Table 1) with no change in the wavelength intensity maximum and no shift. The quantum yield of the phosphoenzyme measured in the same conditions was 0.22 as compared to 0.27 for the nonphosphorylated enzyme. Conversely, the fluorescence of the phosphorylated enzyme increased upon ADP addition (Figure 4) and this increase was saturable as expected from the complete dephosphorylation of the enzyme upon transfer of phosphate to the acceptor ADP according to eq 1B.

Given that the fluorescence of Trp-137 in NDP kinase depends on phosphorylation on the catalytic histidine, this change can be used to monitor the equilibrium of the enzyme reaction with nucleotides (eq 1A). NDP kinase was incubated with a mixture of ADP and ATP in variable ratio, but the total amount of nucleotides was kept constant and in excess relative to protein concentration. The equilibrium was attained almost instantaneously. The fluorescence increases by 22% from a low intensity corresponding to NDP kinase in the presence of an excess of ATP, to a higher intensity, representative of the enzyme in the presence of an excess of ADP (Figure 5). The observed fluorescence is assumed to be the sum of the contributions of phosphorylated (E-P) and nonphosphorylated enzyme (E) by neglecting other possible nucleotide−protein complexes [the fluorescent signal of E and of the complex (E-ADP) are similar]. Since no cooperativity is apparent, the data can be fitted to a hyperbolic function (Figure 5). The half-transition corresponds to half of the phosphorylation of the protein and is found for a ratio [ADP]/[ATP] = 0.19. This ratio measures the equilibrium constant of nucleotides with NDP kinase, according to

$$K_{eq} = \frac{[\text{E-P}][\text{ADP}]}{[\text{E}][\text{ATP}]} \qquad (9)$$

The value derived from Figure 5 (K_{eq} = 0.19) is similar to the equilibrium constant of yeast NDP kinase with nucleotides (Garces & Cleland, 1969) as evaluated from the kinetics parameters according to Haldane relationships. Lascu *et al.* (1983) reported a similar value for phosphorylation of pig heart NDP kinase by ATP by monitoring the amount of produced ADP.

Addition of ATP also modifies the time-resolved fluorescence properties of NDP kinase. In a saturating amount at 20 °C, ATP decreases the mean lifetime of NDP kinase fluorescence by 19% (Figure 2b, Table 1). This is due to a decrease of the amplitude of the major component (4.5 ns) and to a reciprocal increase of the minor component (3.4 ns) with both lifetimes reaching comparable preexponential values (Figure 2b, Table 1). In contrast, addition of ADP has very little effect on the fluorescence mean lifetime of the enzyme (3%) (not shown).

A similar experiment was performed with the phosphorylated enzyme at 3 °C, in order to stabilize the molecule during acquisition of the data. Figure 6 and Table 3 show the lifetime distribution for NDP kinase obtained under these conditions, alone (Figure 6a) or in the presence of ATP (Figure 6b). Data obtained with the phosphorylated enzyme alone (Figure 6d) or in the presence of ADP (Figure 6c) are also shown. The experiments display the same pattern of lifetime distributions, with some quantitative variations (Table 3). The fluorescence decay of the free enzyme was almost monoexponential at both 3 and 20 °C. Addition of ATP decreases the mean lifetime by 11% (from 4.77 to 4.25 ns), due to a decrease of the lifetime of the major component (from 5.2 to 4.9 ns). In the cold, however, the splitting of the signal by ATP is not so clear, appearing as an unresolved shoulder. The striking similarity of lifetimes distribution for the phosphoenzyme (Figure 6d) and for the enzyme in the presence of excess ATP (Figure 6b) confirms that the signal

Table 1: Effect of Phosphorylation on Intensity Decay Parameters of NDP Kinase at 20 °C[a]

NDP kinase	QY	mean lifetime (ns)	τ_1 (ns)	c_1 (%)	τ_2 (ns)	c_2 (%)	τ_3 (ns)	c_3 (%)	κ^2
wt	0.27	4.36	4.6	90	3.4	4	0.3	6	1.18
wt + ATP	0.22	3.66	4.5	44	3.3	49	0.3	7	1.03
H55A	0.37	6.0	6.8	86	3.3	5	0.2	9	1.03
H55A + ATP		6.2	6.8	89	3.3	4	0.3	7	1.06

[a] Quantum yields (QY), mean lifetimes, lifetimes (τ_i), and their relative amplitudes (c_i) for wild-type and the H55A mutant NDP kinase at 20 °C are shown. The same experiment is shown in Figure 2.

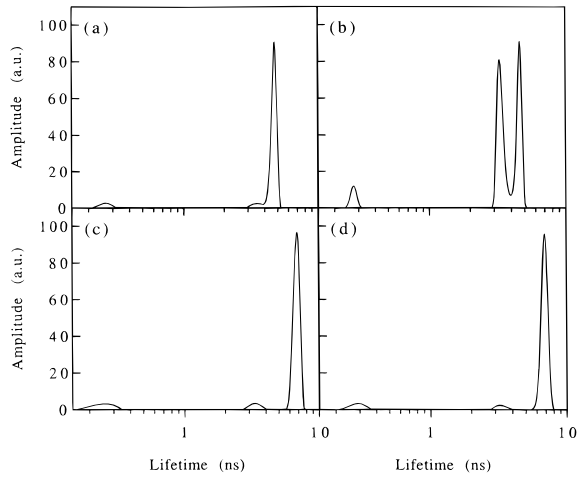

FIGURE 2: Fluorescence lifetimes at 20 °C. Fluorescence decays distribution for wild-type (a, b) and H55A (c, d) NDP kinase at 20 °C in the absence (a, c) or in the presence (b, d) of ATP. Protein concentration was 20 μM, and nucleotides were made 0.5 mM in buffer T .

Table 2: Parameters of the Fluorescence Anisotropy Decays of NDP Kinase and Some Mutants at 20 °C

	Θ_1 (ns)	A_1 (%)	Θ_2 (ns)	A_2 (%)	r_0	κ^2
NDPK	68 ± 20	100			0.276	1.16
NDPK-P	70 ± 20	100			0.277	1.03
H55A	61 ± 20	99.2	2.3 ± 0.1	0.8	0.273	1.09
P105G	64 ± 30	96	7.0 ± 1.0	4	0.274	1.06

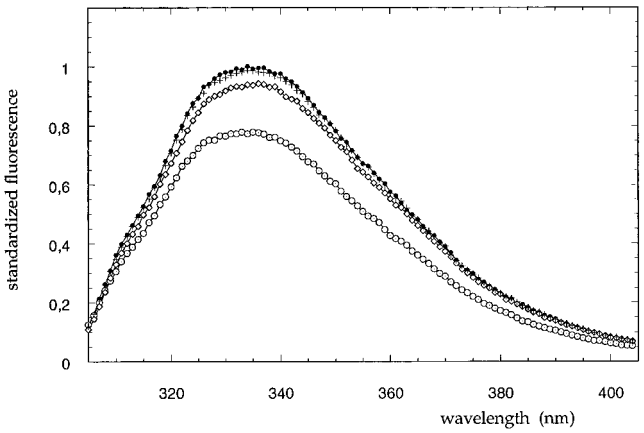

FIGURE 3: Fluorescence emission spectra of wild-type NDP kinase in the presence of various nucleotides. Wild-type NDP kinase (2 μM subunit) was incubated in buffer T with saturating amounts of nucleotides: (▲) no addition, (+) with 0.5 mM AMP-PCP or AMP-PNP, (◇) with 0.5 mM ADP, and (○) with 0.5 mM ATP.

of the enzyme in the presence of ATP reflects the formation of the phosphohistidine. After addition of ADP to the phosphoenzyme, the mean lifetime increases to the value obtained with unphosphorylated enzyme.

Experiments performed at different emission wavelengths (320 and 380 nm) gave similar patterns of lifetime distributions, indicating that an excited-state reaction is unlikely (data not shown).

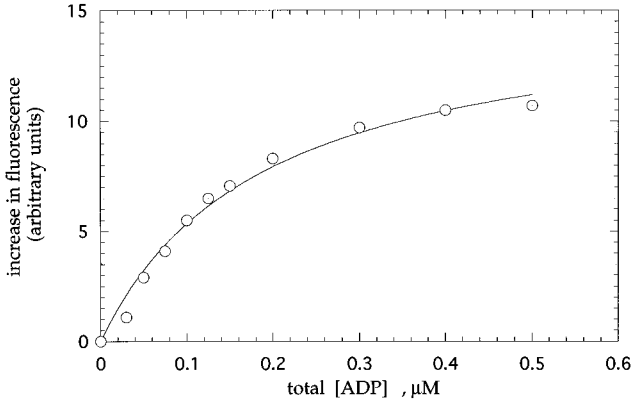

FIGURE 4: Dephosphorylation of the phosphorylated intermediate monitored by fluorescence. The fluorescence of phosphorylated NDP kinase (0.4 μM subunit) was measured in buffer T (λ_{exc} = 295 nm, λ_{em} = 335 nm) as a function of increasing amounts of ADP.

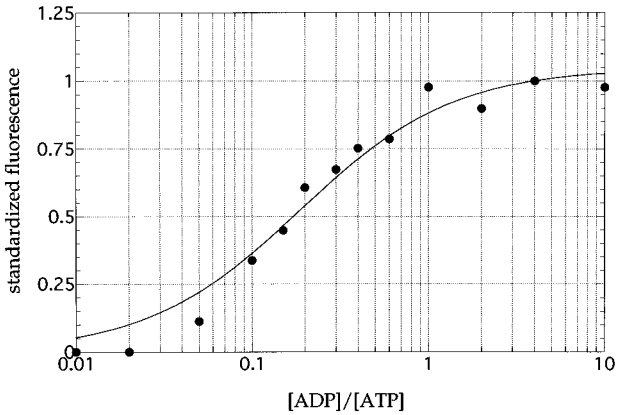

FIGURE 5: Intrinsic fluorescence of NDP kinase as a function of the ratio [ADP]/[ATP]. Wild-type NDP kinase (1.8 μM subunit) in buffer T was incubated at the equilibrium with ATP and ADP (total amount of nucleotides = 25 μM, in varying [ADP]/[ATP] ratio). Data were fitted to eq 8, modified to the following formulation $\Delta F = \Delta F_{max} r/(r + K_{eq})$, where r = [ADP]/[ATP], ΔF_{max} is the maximum variation in fluorescence, and ΔF is the variation observed at a given ratio r. The value for K_{eq} is 0.19 ± 0.02. The hyperbolic function appears here as a sigmoid due to the logarithmic representation of the x-axis.

Structural Basis for the Fluorescence Change Induced by Phosphorylation. X-ray diffraction data show that Trp-137 does not belong to the first shell of residues in direct contact with the catalytic His-122 and enzyme phosphorylation is not expected to directly modify the environment of the Trp-137. However, the His-55 side chain is found in close proximity to both Trp-137 and His-122 (Figure 7). Although His-55 is totally conserved in eukaryotic NDP kinases, previous studies did not indicate that it might play a role in the catalytic mechanism (Tepper *et al.*, 1994).

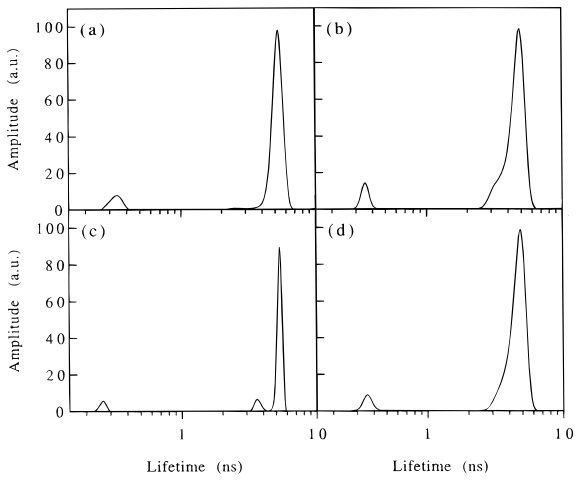

FIGURE 6: Fluorescence lifetimes at 3 °C. Fluorescence decays distribution of NDP kinase at 3 °C. Protein concentration was 20 μM for the enzyme in panels a and b, as well as for the phosphorylated enzyme in panels c and d. In panel b is shown the enzyme with ATP; in panel c, the phosphorylated enzyme with added ADP.

H55A mutant NDP kinase was prepared by site-directed mutagenesis and purified to homogeneity as a hexameric protein. Table 4 shows the kinetic parameters of H55A mutant NDP kinase computed from initial rate studies performed at a constant [dTDP]/[ATP] ratio (Segel, 1975), as compared to those of the wild-type enzyme. Although the k_{cat}/K_M does not vary significantly, the K_M and k_{cat} of the mutant protein are both reduced. However, the residual 20% catalytic activity strongly argues against His-55 being directly involved in phosphotransfer. H55A protein has altered stability with a T_m of 45 °C as compared to 55 °C for the wild-type enzyme. Similarly, the H55A enzyme is denatured at a lower urea concentration (half transition occurring at 3.75 M urea) than for wild-type enzyme (5.5 M urea) (data not shown).

The fluorescence emission spectrum of the H55A protein is shown in Figure 1. The quantum yield increases relative to that of wild type by about 40% (Table 1), without either distortion of the spectrum or shift of the maximum. However, the H55A mutant fluorescence is unaffected by phosphorylation since less than 5% variation is detected upon addition of saturating levels of ATP, ADP, AMP-PCP, or AMP-PNP (results not shown).

The fluorescence decay of H55A mutant protein (Figure 2c, Table 1) is also mostly monoexponential with a mean lifetime of 6 ns as compared to 4.4 ns for wild-type enzyme. The mean decay times are proportional to their respective quantum yields as expected from similar radiative constants (De Lauder & Wahl, 1970). The fluorescence anisotropy decay of H55A mutant protein gives a long correlation time of 61± 10 ns, similar to that of the wild-type protein and consistent with its hexameric structure. A slightly reduced value observed reproducibly for the anisotropy extrapolated at zero time suggests, however, a slight increase in the rotational dynamics of Trp-137 in this mutant.

When ATP is added to the His-55 mutant protein, no significant difference in the distribution of lifetimes is observed (Figure 2d, Table 1), again showing that in the absence of the His-55 side chain, the fluorescence of Trp-137 is not modified by the phosphohistidine.

DISCUSSION

Environment of the Trp-137 Residue in NDP Kinase. The steady-state fluorescence properties of the single Trp-137 are consistent with those of a relatively buried residue (Burstein *et al.*, 1973), in agreement with the three-dimensional structure of *Dictyostelium* NDP kinase. Indeed, the solvent-accessible area of the indole ring of Trp-137 is 9.6 Å^2 (Morera *et al.*, 1994a) as compared to 266 Å^2 (probe radius, 1.4 Å^2) for the total accessible area of a tryptophan side chain. Trp-137 is remote from the His-122 phosphorylation site by 7−10 Å and its polar NH group is involved in a hydrogen bond to Nδ of His-55 (distance = 2.6 Å). His-55 is also buried with only 2.5 Å^2 of accessible surface (Morera *et al.*, 1994a). There is no hydrogen bonding with the -NH indole of Trp-137 in the H55A mutant (Figure 7) and this results in a 40% increase in the quantum yield (QY = 0.37) and in the decay constant (τ = 6.0 ns). We conclude that the fluorescence of Trp-137 in the native wild-type enzyme is strongly quenched by His-55. Tryptophan−histidine interactions have been studied in proteins like barnase (Loewenthal *et al.*, 1991; Willaert *et al*., 1992), in peptides like anantin, and in other model systems (Shinitzky & Goldman, 1967; Vos *et al*., 1994). It is generally assumed that the protonated form of histidine is a more efficient quencher (Willaert *et al.*, 1992). However, in the folded form of the enzyme, His-55 is likely to be unprotonated since its Nδ shares a hydrogen bond with the nitrogen of Trp-137. According to preliminary studies of the pH dependence of the NDP kinase intrinsic fluorescence, no titration can be observed in the 5−9 pH range (results not shown). The destabilization of the hexamer in urea or at low temperatures in the H55A mutation also indicates that His-55 exists in a favorable hydrophobic environment which stabilizes the folded conformation in the wild-type enzyme.

It is remarkable that the fluorescence decay parameters of NDP kinase are quasi-monoexponential. Several examples of monoexponential or nearly monoexponential decays of a single Trp residue have been reported for various proteins (Chen *et al*., 1987; Willaert *et al*., 1992; Brochon *et al*., 1993; Blandin *et al*., 1994). They are usually observed for residues which are strongly immobilized on the picosecond and nanosecond time scales, as indicated by their corresponding fluorescence anisotropy decays. This is also the case of NDP kinase from *Dictyostelium* reported here. The homogeneity of the fluorescence lifetime is usually associated with a lack of flexibility of the protein matrix around the indole ring at all time scales above the nanosecond range. In addition, the single lifetime of Trp-137 is indicative of a similar microenvironment for the six tryptophans within the hexamer and agrees with the absence of induced cooperative interactions between active sites. The single correlation time of 65 ns obtained from the anisotropy decays, and the total absence of a nondepolarizing amplitude in the decays, also demonstrate that the NDP kinase solution is highly monodispersed and consists of the pure hexameric protein under the conditions used. These properties are mostly conserved in the mutant H55A protein, indicating that the removal of the hydrogen bond between His-55 and Trp-137 does not confer large conformational freedom to the tryptophan side chain.

Phosphorylation of NDP Kinase upon ATP Binding. The fluorescence intensity and the mean lifetime of the Trp-137

Table 3: Effect of Phosphorylation and Dephosphorylation on Intensity Decay Parameters of NDP Kinase at 3 °C[a]

	mean lifetime (ns)	τ_1 (ns)	c_1 (%)	τ_2 (ns)	c_2 (%)	τ_3 (ns)	c_3 (%)	κ^2
wt NDPK	4.77	5.2	91	2.6	1	0.3	8	1.07
wt NDPK + ATP	4.25	4.9	93	nr		0.4	7	1.06
wt NDPK-P	4.34	4.9	94	nr		0.4	6	1.19
wt NDPK-P + ADP	4.80	5.3	85	3.6	8	0.3	7	1.12

[a] Same experiment as in Figure 6: The enzyme concentration, whether phosphorylated or not, is 20 μM (in subunits) in buffer T. ATP = 5 mM, ADP = 5 mM. nr, not resolved.

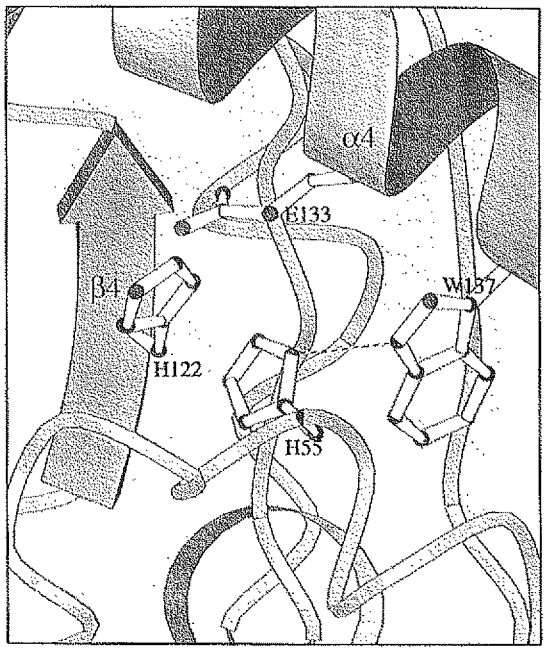

FIGURE 7: Environment of Trp-137 in NDP kinase. View of the active site in a subunit of *Dictyostelium* NDP kinase. His-122 interacts with Glu-133 on top. Trp-137 is located in the last turn of helix α_4 and its nitrogen is hydrogen-bonded with Nδ of His-55, which belongs to helix α_A. His-122 and His-55 are in van der Waals contact.

Table 4: Effect of His-55 Mutation on Kinetic Parameters of *Dictyostelium* NDP Kinase[a]

	wild-type	H55A
specific activity (units/mg)	2000	400
k_{cat} (s^{-1})	500	120
K_M^{ATP} (mM)	0.44	0.11
K_M^{dTDP} (mM)	0.11	0.04
k_{cat}/K_M^{ATP} (M^{-1} s^{-1})	0.67×10^7	0.65×10^7
k_{cat}/K_M^{dTDP} (M^{-1} s^{-1})	2.7×10^7	1.8×10^7

[a] The catalytic rate constants (k_{cat}) and Michaelis constants (K_m) were obtained from initial rate measurements at constant ratio of nucleotide concentrations: [dTDP]/[ATP]= 0.05, 0.067, and 0.1 with [ATP] varying from 0.2 to 2 mM. The specific activity is expressed in units/mg (1 unit is the amount of enzyme catalyzing the transfer of 1 μmol of phosphate/min).

are both decreased by about 20% at 20 °C in the presence of ATP or in the phosphoenzyme. As no important difference is seen between the structures of the phosphohistidine intermediate and the free enzyme (Morera *et al.*, 1995a), this fluorescence quenching is probably due to a small conformational change, undetected by X-ray studies, which may be related to the dynamics of the protein. The location of residue His-55 explains its crucial role in the detection of the phosphate moiety on the catalytic histidine. We hypothesize that the phosphate group causes a constraint on the His-55 side chain which results in an increase in Trp-137 quenching. In the absence of the His-55 imidazole ring, the fluorescence decay of Trp-137 is insensitive to His-122 phosphorylation although the protein is active. Therefore, the imidazole ring of His-55 participates in Trp-137 anchorage in the protein matrix and also functions as a sensitive relay between His-122 and Trp-137.

The decreased mean lifetime of phosphoenzyme fluorescence is due to the appearance at 20 °C of a shorter decay time (3.4 ns) in addition to the 4.5-ns decay found for free NDP kinase. The relative amplitudes of both components strongly depend upon the temperature (Figures 2 and 6). The two components observed for the phosphoenzyme are indicative of a heterogeneity in the microenvironment of Trp-137 which does not exist in the free enzyme. Heterogeneity in fluorescence decays is frequently reported even for single-tryptophan proteins [reviewed in Fetler *et al.* (1992)], and its significance is a matter of controversy. A specific reaction of the excited state occurring on the nanosecond time scale is unlikely, since the fluorescence kinetics were not dependent on the emission wavelength from 320 to 380 nm , and since no evidence was found for a negative amplitude in the decay over this wavelength range (Brand & Laws, 1980). On the other hand, half-of-the-sites reactivity was never observed in the phosphohistidine intermediate formation, either from biochemical ((Lascu *et al.*, 1983; this study) or X-ray studies (Morera *et al.*, 1995a), and it cannot be put forward to explain the splitting of the signal upon phosphorylation. Another explanation is the occurrence of a slow equilibrium in the microenvironment of Trp-137 in the phosphorylated protein. If the hypothesis of a chemical equilibrium is considered, both states are equally represented and could be due to either the ionization of the phosphate group or that of a neighboring protonated residue. However, preliminary studies with steady-state fluorescence show no significant pH dependence in the 5−10 pH range for the phosphoenzyme as for the non-phosphoenzyme.

Multiexponential fluorescence intensity decays have generally been interpreted as arising from conformational heterogeneity of the protein in solution (Szabo & Rayner, 1980; Royer, 1993). They could reveal either the existence of distributions of conformational substates (Alcala *et al.*, 1987) or the presence of discrete species undergoing slow exchange (Merola *et al.*, 1989; Blandin, 1994). The existence of the two signals for Trp-137 (4.5 and 3.6 ns) could be related to a slow equilibrium of phosphoenzyme between two conformations. A structural variation of a hinge-type motion for the helices of α_A and α_2, at the surface of the protein, has been reported and seems to participate in nucleotide binding (Webb *et al.*, 1995). As His-55 is itself located in helix α_A, it is tempting to speculate that, in the phosphoenzyme, this exposed subdomain of NDP kinase oscillates between two conformations related to release or entrance of the nucleoside diphosphate, resulting in a

different quenching of Trp-137 fluorescence. Further experiments are necessary to identify the individual steps in the catalytic cycle, release of the first product and binding of the second substrate, and to clarify the reason for Trp-137 lifetime heterogeneity in the phosphorylated enzyme.

ACKNOWLEDGMENT

We thank Joel Janin and his collaborators from the Laboratoire d'Enzymologie et Biochimie Structurales (Gif-sur-Yvette, France), Jeffrey Stock (Princeton University), and Pascal Garcia, Philippe Minard, and Jeannine Yon-Kahn (Université Paris-Sud) for helpful and stimulating discussions. We appreciate the technical staff of LURE for running the synchrotron machine and computing facilities.

REFERENCES

Alcala, J. R., Gratton, E., & Prendergast, F. G. (1987) *Biophys. J. 51*, 925−936.
Blandin, P., Merola, F., Brochon, J. C., Tremeau, O., & Menez, A. (1994) *Biochemistry 33*, 2610−2619.
Bominaar, A. A., Tepper, A. D., & Véron, M. (1994) *FEBS Lett. 353*, 5−8.
Brand, L., & Laws, W. R. (1980) in *Time resolved fluorescence spectroscopy in biochemistry and biology* (Cundall, R. B., & Dale, R. E., Eds.) pp 319−340, Plenum Publishing Corp., New York.
Brochon, J. C., Tauc, P., Mérola, F., & Schoot, B. M. (1993) *Anal. Chem. 65*, 1028−1034.
Burstein, E. A., Vedenkina, N. S., & Ivkova, M. N. (1973) *Photochem. Photobiol. 18*, 263−279.
Chen, L. X.-Q., Longworth, J. W., & Fleming, G. R. (1987) *Biophys. J. 51*, 865−873.
Cherfils, J., Morera, S., Lascu, I., Véron, M., & Janin, J. (1994) *Biochemistry 33*, 9062−9069.
Chiadmi, M., Moréra, S., Lascu, I., Dumas, C., LeBras, G., Véron, M., & Janin, J. (1993) *Structure 1*, 283−293.
De Lauder, W. B., & Wahl, P. (1970) *Biochemistry 9*, 2750−2754.
Dearolf, C. R., Hersperger, E., & Shearn, A. (1988) *Dev. Biol. 129*, 159−168.
Dumas, C., Lascu, I., Moréra, S., Glaser, P., Fourme, R., Wallet, V., Lacombe, M.-L., Véron, M., & Janin, J. (1992) *EMBO J. 11*, 3203−3208.
Fetler, L., Tauc, P., Hervé, G., Ladjimi, M. M., & Brochon, J. C. (1992) *Biochemistry 31*, 12504−12513.
Garces, E., & Cleland, W. W. (1969) *Biochemistry 8*, 633−640.
Gilles, A. M., Presecan, E., Vonica, A., & Lascu, I. (1991) *J. Biol. Chem. 266*, 8784−8789.
Kouyama, T., Kinosita, K., & Ikegami, A. (1989) *Eur. J. Biochem. 182*, 517−512.
Kunkel, T. A. (1985) *Proc. Natl. Acad. Sci. U.S.A. 82*, 488−492.
Lacombe, M.-L., Wallet, V., Troll, H., & Véron, M. (1990) *J. Biol. Chem. 265*, 10012−10018.
Lascu, J., Pop, R. D., Porumb, H., Presecan, E., & Proinov, I. (1983) *Eur. J. Biochem. 135*, 497−503.
Lascu, I., Chaffotte, A., Limbourg-Bouchon, B., & Véron, M. (1992) *J. Biol. Chem. 267*, 12775−12781.
Lascu, I., Deville-Bonne, D., Glazer, P., & Véron, M. (1993) *J. Biol. Chem. 268*, 20268−20275.
Lascu, I., Deville-Bonne, D., Glazer, P., & Véron, M. (1994) *J. Biol. Chem. 269*, 7046.
Lecroisey, A., Lascu, I., Bominaar, A., Véron, M., & Delepierre, M. (1995) *Biochemistry 34*, 12445−12450.
Livesey, A. K., & Brochon, J. C. (1987) *Biophys. J. 52*, 693−706.
Loewenthal, R., Sancho, J., & Fersht, A. R. (1991) *Biochemistry 30*, 6775−6779.
Merola, F., Blandin, P., Brochon, J. C., Trémeau, O., & Ménez, A. (1995) *J. Fluoresc. 5*, 205−215.
Mérola, F., Rigler, R., Holmgren, A., & Brochon, J. C. (1989) *Biochemistry 28*, 3383−3398.
Moréra, S., Dumas, C., Lascu, I., Lacombe, M.-L., Véron, M., & Janin, J. (1994a) *J. Mol. Biol. 243*, 873−890.
Moréra, S., Lascu, I., Dumas, C., LeBras, G., Briozzo, P., Véron, M., & Janin, J. (1994b) *Biochemistry 33*, 459−467.
Moréra, S., Chiadmi, M., Lascu, I., & Janin, J. (1995a) *Biochemistry 34*, 11062−11070.
Moréra, S., Lacombe, M.-L., Yingwu, X., LeBras, G., & Janin, J. (1995b) *Structure 3*, 1307−1314.
Munoz-Dorado, J., Inouye, M., & Inouye, S. (1990) *J. Biol. Chem. 265*, 2702−2706.
Parker, C. A., & Rees, W. T. (1960) *Analyst 85*, 587−600.
Parks, R. E. J., & Agarwal, R. P. (1973) *The Enzymes 8*, 307−334.
Rosengard, A. M., Krutzsch, H. C., Shearn, A., Biggs, J. R., Barker, E., Margulies, I. M. K., King, C. R., Liotta, L. A., & Steeg, P. S. (1989) *Nature 342*, 177−180.
Royer, C. A (1993) *Biophys. J. 65*, 9−10.
Segel, I. H. (1975) *Enzyme kinetics*, pp 608−612, John Wiley & Sons, Inc.
Shinitzky, M., & Goldman, R. (1967) *Eur. J. Biochem. 3*, 139−144.
Steeg, P. S., Bevilacqua, G., Kopper, L., Thorgeirsson, U. P., Talmadge, J. E., Liotta, L. A., & Sobel, M. E. (1988) *J. Natl. Cancer Inst. 80*, 200−204.
Szabo, A. G., & Rayner, D. M. (1980) *J. Am. Chem. Soc. 102*, 554−563.
Tepper, A., Dammann, H., Bominaar, A. A., & Véron, M. (1994) *J. Biol. Chem. 269*, 32175−32180.
Valeur, B., & Weber, G. (1977) *Photochem. Photobiol. 25*, 441−444.
Vos, R., & Engelborghs, Y. (1994) *Photochem. Photobiol. 60*, 24−32.
Wahl, P. (1980) in *Time resolved fluorescence spectroscopy in biochemistry and biology* (Cundall, R. B., & Dale, R. E., Eds.) pp 497−521, Plenum Publishing Corp., New York.
Wallet, V., Mutzel, R., Troll, H., Barzu, O., Wurster, B., Véron, M., & Lacombe, M.-L. (1990) *J. Natl. Cancer Inst. 82*, 1199−1202.
Webb, P. A., Perisic, O., Mendola, C. E., Backer, J. M., & Williams, R. L. (1995) *J. Mol. Biol. 251*, 574−587.
Werner, T. C., & Foster, L. S. (1979) *Photochem. Photobiol. 29*, 905−914.
Willaert, K., Loewenthal, R., Sancho, J., Froeyen, M., Fersht, A., & Engelborghs, Y. (1992) *Biochemistry 31*, 713−716.
Williams, R. L., Oren, D. A., Munoz-Dorado, J., Inouye, S., Inouye, M., & Arnold, E. (1993) *J. Mol. Biol. 234*, 1230−1247.

BI960945M